Available online at www.sciencedirect.com
SCIENCE DIRECT®
PERGAMON
Polyhedron 22 (2003) 1135–1146
POLYHEDRON
www.elsevier.com/locate/poly

Synthesis, acid–base and coordination properties towards Cu(II), Zn(II), and Cd(II) ions of two new polyamino-phenolic ligands, including the crystal structure of a fully protonated ligand

Gianluca Ambrosi [a], Mauro Formica [a], Vieri Fusi [a,*], Luca Giorgi [a], Annalisa Guerri [b], Mauro Micheloni [a,*], Roberto Pontellini [a], Patrizia Rossi [b]

[a] *Istituto di Scienze Chimiche, Università di Urbino, P.zza Rinascimento 6, I-61029 Urbino, Italy*
[b] *Dipartimento di Energetica 'S. Stecco', Università di Firenze, via S. Marta 3, I-50139 Firenze, Italy*

Received 26 November 2002; accepted 17 January 2003

Abstract

The synthesis of the two new ligands 2,6-bis{[bis-(2-aminoethyl)ethylamino]methyl}phenol (**L1**) and bis{[2(2-aminoethylamino)ethylamino]methyl}phenol (**L2**) is reported. Both ligands have two diethylenetriamine subunits separated by two phenolic spacers; the simple phenol is present in the framework of **L1**, while the longer 4,4′-bis(1-phenol) is in **L2**. The acid–base behavior of both ligands in aqueous solution was studied by potentiometry (25 °C, $I = 0.15$ mol dm^{-3}, NaCl). As a neutral molecule, **L1** behaves as hexaprotic base and as monoprotic acid, **L2** behaves as hexaprotic base and as diprotic acid. The stability constants for their Cu(II), Zn(II), and Cd(II) complexes were determined by potentiometry and UV–Vis experiments under the same experimental conditions and compared. Both ligands form stable mono- and dinuclear complexes. The analysis of the data revealed a similar coordination arrangement in the mononuclear complexes, while a different arrangement is suggested for the dinuclear one. The role of the phenol and of the 4,4′-bis(1-phenol) as spacers of two amine functions in metal ion coordination is discussed. The crystal structure of the fully protonated species of **L1** (**L1**·6HBr) is reported and discussed.

Keywords: Synthesis; Equilibria; Dinuclear complexes; Polyamines; Phenol; Crystal structure

1. Introduction

Dinuclear transition metal complexes and ligands capable of yielding them have been attracting increasing attention in the field of synthetic and biological chemistry due to the key roles they play in many applications [1–5]. They are used as model systems for the active centers of many metalloenzymes [6–8], as devices with which to host and carry small molecules or ions and as catalysts [9–12]. In fact, dinuclear metal complexes have been used successfully for the recognition and assembly of external species of different nature such as inorganic and organic substrates [13]. For this reason, the synthesis of ligands able to form dinuclear complexes is of great interest.

The most important factors for the coordination and/or activation of a coordinated secondary species are an unsaturated coordination environment of the two metals, the nature of the two metal ions and the preorganization of the receptor to host the new species. The distance between the two metal ions is crucial to allow the cooperation of both metal ions in forming the active center present for example, in oxygen receptors, activators and carriers.

Dinuclear hosts are often obtained using macrocyclic ligands with a high number of donor atoms and, usually, the transition metal ions 'impose' the ligand arrangement fixed by the coordination requirement of the ions. Recently, some non-cyclic ligands have been reported [14] and, among these, ligands containing a phenolic

* Corresponding authors. Fax: +39-0722-350032.
E-mail address: vieri@chim.uniurb.it (V. Fusi).

0277-5387/03/$ - see front matter
doi:10.1016/S0277-5387(03)00099-8

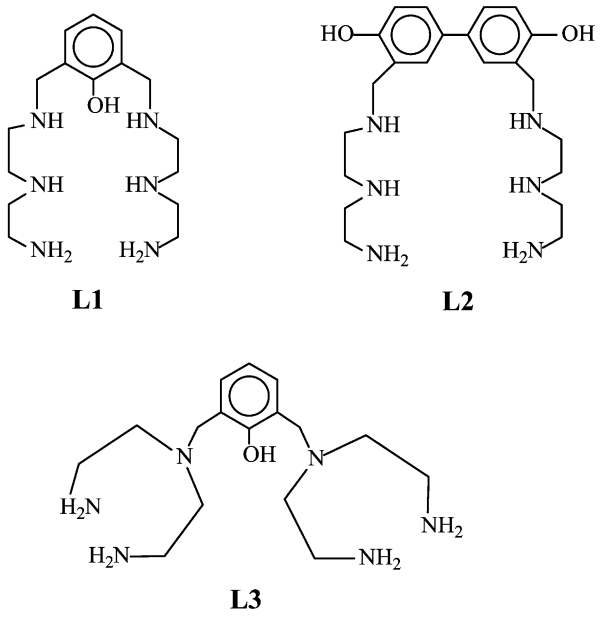

Fig. 1. Ligands.

moiety in a binding skeleton, as **L3** [13a] (see Fig. 1), has attracted considerable attention.

This ligand shows two separate triamine binding subunits linked together by a phenol group; it is capable of assembling two transition metal ions close to each other and thus of forming simple and stable unsaturated dinuclear complexes with various transition metal ions. The dinuclear complexes become excellent hosts, depending upon the metals, for molecules such as dioxygen, azide, imidazole, chloride and others. All the adducts formed show the same coordination environment in which the two metal ions cooperate to assemble the guest, which is bound in a bridge disposition by the two metal ions.

To learn more about the structural parameters needed to obtain a bimetallic center using simple amine units, we designed the two new ligands **L1** and **L2** (see Fig. 1). In both ligands, two diethylenetriamine units are separated by different aromatic moieties. The two subunits are linked to the aromatic part on a terminal amine function. The two aromatic parts are the phenol (PH) and the 4,4′-bis(1-phenol) (BPH) groups, for **L1** and **L2**, respectively. It should be underlined that **L1** is a structural isomer of **L3**; moreover, both ligands contain a chromogenic group which can be exploited as optical sensor. An extensive synthesis of **L1**, which has been already published in brief [15], and of **L2** are reported. The acid–base behavior and the coordination properties toward some M(II) transition cations of the ligands were determined and are reported.

2. Experimental

2.1. Synthesis

The synthesis of ligands **L1** and **L2** was obtained following the procedures reported in Schemes 1 and 2. 1-Benzyloxycarbonyl-1,4,7-triazaheptane (**1**), and 2,6-diformyl-anisole (**2**) were prepared as previously described [16,17]. Solvents and starting materials were used as purchased.

2.1.1. 2,6-Bis[2(2-benzyloxycarbonylaminoethyl)ethylamino]anisole (3)

Over a period of 3 h, a solution of **2** (1.64 g, 0.01 mol) in 100 cm^3 of chloroform was added to a solution of **1** (4.74 g, 0.02 mol) in 200 cm^3 of chloroform containing

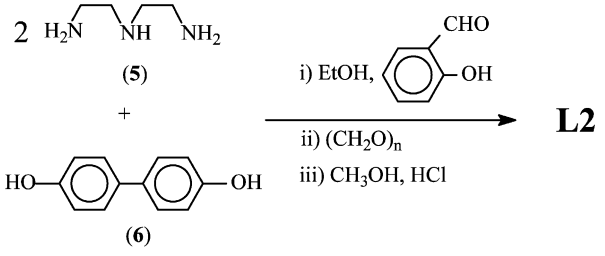

Scheme 2. Synthetic pathway followed to obtain compound **L2**.

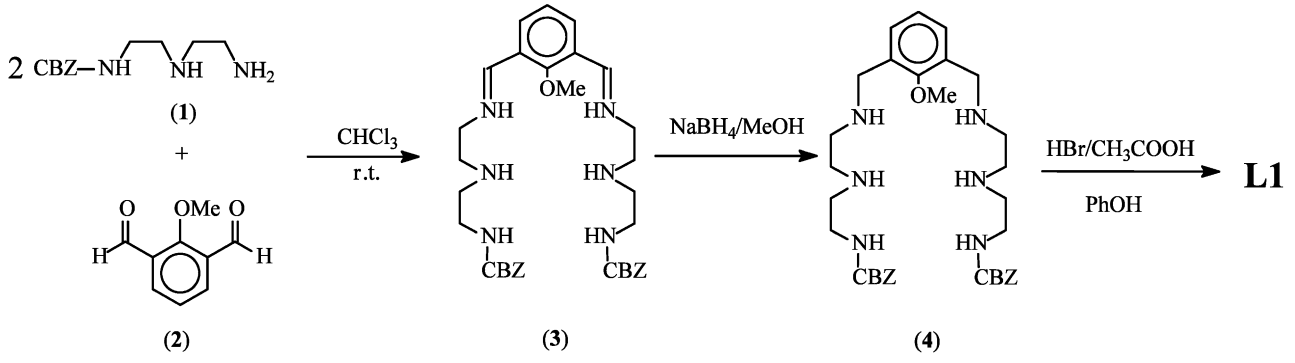

Scheme 1. Synthetic pathway followed to obtain compound **L1**.

molecular sieves at room temperature. The reaction mixture was maintained under stirring for a further 3 h. Subsequently, the mixture was filtered and the solution was evaporated under reduced pressure. The yellow solid obtained was recrystallized from hot CH_3CN obtaining **3** (5.67 g, 94%; ^{1}H NMR $CDCl_3$, 25 °C: 2.39 (t, 4H), 3.27 (m, 8H), 3.84 (m, 7H), 5.07 (s, 4H), 7.33 (m, 10H), 7.48 (t, 1H), 7.88 (d, 2H), 8.62 (s, 2H) ppm. FT-IR 1635 (HC=N), 1706 (C=O) cm^{-1} *Anal.* Calc. for $C_{33}H_{42}N_6O_5$: C 65.76; H 7.02; N 13.94. Found: C 65.9; H 6.9; N 14.0.

2.1.2. 2,6-Bis{[2(2-benzyloxycarbonylaminoethyl)ethylamino]methyl}anisole (*4*)

The schiff-base **3** (3.01 g, 5 mmol) was dissolved in 200 cm^3 of methanol to which a small portion of $NaBH_4$ (0.47 g, 12.5 mmol) was then added under stirring. The reaction mixture was maintained under stirring for 12 h, then filtered and evaporated under reduced pressure to give a white solid. The solid was dissolved in a minimum amount of ethanol and to the solution obtained, HBr was slowly added to obtain a strongly acid solution and thus destroy the excess $NaBH_4$. Diethylether was added to this solution until complete precipitation of **4** as tetrahydrobromide salt (3.53 g, 76%). ^{1}H NMR D_2O, pH 2, 25 °C: 3.18 (t, 4H), 3.41 (m, 12H), 3.80 (s, 3H), 4.34 (s, 4H), 5.03 (s, 4H), 7.29 (t, 1H), 7.34 (m, 10H), 7.52 (d, 2H) ppm. ^{13}C NMR 38.2, 44.3, 44.4, 47.9, 49.5, 64.2, 68.6, 126.0, 127.4, 129.2, 129.8, 130.1, 134.7, 137.4, 158.7, 159.9 ppm. *Anal.* Calc. for $C_{33}H_{50}Br_4N_6O_5$: C 42.60; H 5.42; N 9.03. Found: C 42.5; H 5.5; N 8.9.

The free molecule **4** was obtained in almost quantitative yield by extracting it with $CHCl_3$ from an alkaline aqueous solution of **4**·4HBr.

2.1.3. 2,6-Bis{[2(2-aminoethylamino)ethylamino]methyl}phenol (*L1*)

4·4HBr (2.79 g, 3 mmol) and phenol (2.82 g, 30 mmol) were dissolved in HBr–CH_3COOH (33%, 50 cm^3). The solution was stirred at 90 °C for 22 h. The resulting suspension was filtered and washed with CH_2Cl_2 several times. The white solid obtained was recrystallized from an EtOH–H_2O mixture to give **L1** as its hexahydrobromide salt (1.75 g, 72%). ^{1}H NMR D_2O, pH 2, 25 °C: 3.32 (t, 4H), 3.41 (t, 4H) 3.48 (m, 8H), 4.32 (s, 4H), 7.02 (t, 1H), 7.41 (d, 2H) ppm. ^{13}C NMR 36.6, 43.8, 44.8, 45.9, 48.6, 121.0, 123.6, 135.2, 155.0 ppm. MS (ESI) (*m*/*z*): 325 ($M+H^+$). *Anal.* Calc. for $C_{16}H_{38}Br_6N_6O$: C 23.73; H 4.73; N 10.38. Found: C 23.7; H 4.7; N 10.3.

2.1.4. 4-Bis{[2(2-aminoethylamino)ethylamino]methyl}phenol] (*L2*)

5 (10.3 g, 0.1 mol) and salicylaldehyde (12.2 g, 0.1 mol) were refluxed together in 150 cm^3 of ethanol for 30 min under stirring. Paraformaldehyde (3.9 g, 0.1 mol) was added to the resulting yellow solution in a small portion. The solution obtained was cooled at room temperature and then added in 1 h to a solution of 6 (9.3 g, 0.05 mol) dissolved in 100 cm^3 of ethanol. The resulting solution was kept under stirring for a further 1 h and then refluxed for 2 h. The cooled mixture was evaporated under reduced pressure to give a brown oil which was then washed with hot hexane (6×20 cm^3). The residue oil was dissolved in ethanol (100 cm^3) and, to the solution obtained 37% HCl was slowly added up to complete precipitation of a white solid which was filtered off and washed with hot methanol to give **L2** as hexa-hydrochloride salt (10.2 g, 32%). ^{1}H NMR D_2O, pH 2, 25 °C: 3.30 (t, 4H), 3.38 (t, 4H) 3.46 (m, 8H), 4.29 (s, 4H), 6.96 (d, 2H), 7.49 (s, 2H), 7.50 (d, 2H) ppm. ^{13}C NMR 36.8, 43.9, 44.7, 45.8, 48.9, 117.3, 118.6, 130.9, 133.3, 155.8 ppm. MS (ESI) (*m*/*z*): 417 ($M+H^+$). *Anal.* Calc. for $C_{22}H_{42}Cl_6N_6O_2$: C 41.59; H 6.66; N 13.23. Found: C 41.7; H 6.5; N 13.1

2.2. X-ray crystallography

L1·6HBr. A $0.4 \times 0.5 \times 0.5$ mm^3 crystal was used for data collection. Intensity data were collected using a Siemens P4 diffractometer with graphite-monochromated Cu Kα radiation ($\lambda = 1.5418$ Å), $T = 298$ K.

Crystal data: $[C_{16}H_{38}N_6O]\cdot 6Br$ (**L1**·6HBr) ($F_w = 809.98$), triclinic, space group $P\bar{1}$, $a = 7.446(2)$, $b = 10.983(3)$, $c = 17.395(4)$ Å, $\alpha = 92.31(2)°$, $\beta = 90.85(2)°$, $\gamma = 95.80(2)°$, $V = 1413.7(6)$ Å^3, $Z = 2$, $D_{calc} = 1.903$ g cm^{-3}, $F(000) = 788$, $\mu = 10.413$ mm^{-1}. The cell constants and the orientation matrix were obtained from a least square fit of 25 centered reflections. Intensities data were corrected for Lorentz and polarization effects. The structure was solved by direct methods using the SIR97 program [18] and refined by full-matrix least squares against F^2 using all data (SHELX97 [19]) to $R_1 = 0.0683$ ($wR_2 = 0.2001$) for 3413 reflections [$I > 2\sigma(I)$] out of 3527 reflections collected in the range $2.5° < \theta < 55°$. An absorption correction was performed with the DIFABS program [20] once the structure was solved. Anisotropic thermal parameters were used for the non H-atoms. With the exception of H(1), which is bound to O1, all the hydrogen atoms were introduced in calculated positions with an overall temperature factor refined to 0.054(4) Å^2. The latter was found in the ΔF map and then refined isotropically.

Geometrical calculations were performed by PARST97 [21] and molecular plots were produced by the program ORTEP3 [22]. Table 1 reports the bond lengths and angles of the cation H_6**L1**$^{6+}$.

Table 1
Bond lengths (Å) and angles (°) for **L1**·6HBr

Bond lengths			
O(1)–C(1)	1.369(9)	C(1)–C(2)	1.41(1)
N(1)–C(8)	1.49(1)	C(2)–C(3)	1.38(1)
N(1)–C(7)	1.50(1)	C(2)–C(7)	1.49(1)
N(2)–C(10)	1.465(9)	C(3)–C(4)	1.39(1)
N(2)–C(9)	1.48(1)	C(4)–C(5)	1.38(1)
N(3)–C(11)	1.47(1)	C(5)–C(6)	1.39(1)
N(4)–C(12)	1.486(9)	C(6)–C(12)	1.52(1)
N(4)–C(13)	1.496(9)	C(8)–C(9)	1.50(1)
N(5)–C(14)	1.50(1)	C(10)–C(11)	1.52(1)
N(5)–C(15)	1.51(1)	C(13)–C(14)	1.49(1)
N(6)–C(16)	1.47(1)	C(15)–C(16)	1.50(1)
C(1)–C(6)	1.40(1)		
Bond angles			
C(5)–C(4)–C(3)	118.5(8)	N(2)–C(10)–C(11)	112.8(6)
C(4)–C(5)–C(6)	121.5(7)	N(3)–C(11)–C(10)	113.6(6)
C(1)–C(6)–C(5)	119.1(7)	N(4)–C(12)–C(6)	111.4(6)
C(1)–C(6)–C(12)	121.4(7)	C(14)–C(13)–N(4)	110.0(6)
C(5)–C(6)–C(12)	119.5(7)	C(13)–C(14)–N(5)	109.4(6)
C(2)–C(7)–N(1)	112.4(6)	C(16)–C(15)–N(5)	111.2(7)
N(1)–C(8)–C(9)	111.2(6)	N(6)–C(16)–C(15)	112.1(7)
N(2)–C(9)–C(8)	109.8(6)		

2.3. General

2.3.1. NMR spectroscopy

^{1}H and ^{13}C NMR spectra were recorded on a Bruker AC-200 instrument, operating at 200.13 and 50.33 MHz, respectively. Peak positions are reported in relation to TMS ($CHCl_3$) or HOD at 4.75 ppm (D_2O). Dioxane was used as reference standard in ^{13}C NMR spectra ($\delta =$ 67.4 ppm).

2.3.2. UV–Vis spectroscopy

UV absorption spectra were recorded at 298 K on a Varian Cary-100 spectrophotometer equipped with a temperature control unit.

2.3.3. Potentiometric measurements

Equilibrium constants for complexation reactions were determined by pH-metric measurements (pH $-$ log $[H^+]$) in 0.15 mol dm^{-3} NaCl at 298.1 $\pm$ 0.1 K, using the fully automatic equipment that has already been described; the EMF data were acquired with the PASAT computer program [23]. The combined glass electrode was calibrated as a hydrogen concentration probe by titrating known amounts of HCl with CO_2-free NaOH solutions and determining the equivalent point by Gran's method [24], which gives the standard potential E° and the ionic product of water ($pK_w =$ 13.83(1) at 298.1 K in 0.15 mol dm^{-3} NaCl, $K_w = [H^+][OH^-]$). Ligand and metal ion concentrations of 1×10^{-3} to 2×10^{-3} were employed in the potentiometric measurements, performing at least three measurements in the pH range 2–11. The HYPERQUAD [25] computer program was used to process the potentiometric data. All titrations were treated either as single sets or as separate entities, for each system, without significant variation in the values of the determined constants.

3. Results and discussion

3.1. Synthesis

The procedure shown in Scheme 1 was followed to obtain **L1**, whereas **1** and **2** were synthesized as previously reported. Compound **1**, in which one of the two primary amine functions of the diethylenetriamine is protected with the benzyloxycarbonyl group (CBZ), was reacted with the dialdehyde **2** in a 2:1 molar ratio by forming the diimine intermediate 3 in high yield. The reaction was carried out in a chloroform solution in the presence of molecular sieves to adsorb the water molecules forming during the reaction. The two imine functions were reduced with $NaBH_4$ in methanol, affording the protected molecule **4**, which was purified as its tetrahydrobromide salt. The methyl and CBZ protective groups of **4** were both removed in 33% HBr in acetic acid in the presence of phenol; with this route it was possible to simultaneously cleave both the CBZ and methyl protective groups, affording **L1** as hexahydrobromide salt, which was recrystallized from a mixture of ethanol–water.

Scheme 2 shows the synthetic route followed to obtain **L2**, which was synthesized in a single multi-step reaction. Compound **5** was mono-protected by the imine function on one of the two primary amine functions of **5** with one equivalent of salicylaldehyde in ethanol. One equivalent of paraformaldehyde was added to this product to form a further imine function. By adding this solution to an ethanol solution of **6**, the insertion of a CH_2–N group in 2- and 2′-position of the aromatic moiety was reached; an acidic medium was used to cleave the protective salicylaldehyde group.

3.2. Description of the crystal structure of *L1*·6HBr

The asymmetric unit contains a molecule of the hexacharged ligand and six bromide ions. Fig. 2 shows an ORTEP view of the compound.

By analyzing the spatial disposition of the side arms, the value of the dihedral angles C2–C7–N1–C8 and C6–C12–N4–C13 were found to be $-70.2(8)$ and 177.3(6)°, respectively, while the expected all-trans arrangement was not found as a consequence of the two main features outlined below.

i) The sequences of the torsion angles for the two polyamine chains are (−sc)–(±ap)–(±ap)–(±

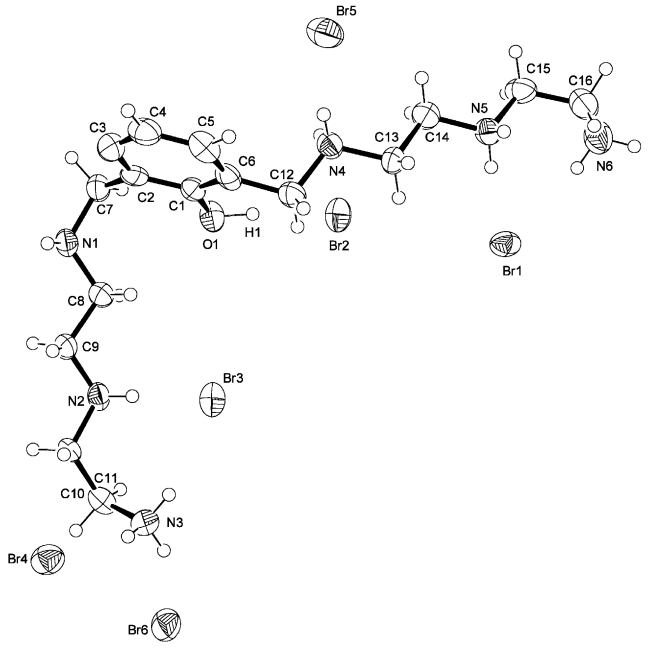

Fig. 2. ORTEP view of compound **L1**·6HBr. The atomic labeling of hydrogens has been omitted. The thermal ellipsoids were drawn with 50% probability.

ap)–(±ap)–(+sc) and (±ap)–(±ap)–(±ap)–(±ap)–(±ap)–(+ac) [26,27] for the chains C7→N3 and C12→N5, respectively. This different arrangement of the two side chains could be related to the disposition of the hydrogen atom bound to the oxygen O1. In fact, the atom H1 points toward the bromide Br2 (H1···Br2: 2.1(1) Å, O1–H1···Br2: 162(10)°) and in this way the lone-pairs of O1 point toward the side chain C7→N3 that arranges itself to optimize the interactions with the oxygen atom, as provided by some C–H···O contacts.As a consequence of the values of the above dihedral angles, the mean plane containing the atoms C12–N4–C13–C14–N5–C15–C16 is quite perpendicular (89.4(3)°) to the aromatic ring, while the mean plane described by the atoms C7–N1–C8–C9–N2–C10–C11 forms an angle of 72.0(3)° with the aromatic ring.The angle between the mean planes containing the two side arms (with the exception of the atoms N3 and N6 which are significantly out of these planes) is 28.2(5)°.

ii) The last dihedral angle defining the conformation of the two polyaminic chains also differs from *anti*-periplanar (ap); in fact it is *syn*-clinal (sc, 86.1(8)°) and *anti*-clinal (ac, 98.4(8)°) for N2–C10–C11–N3 and N5–C15–C16–N6, respectively. This arrangement allows the hydrogen atoms bound to N2 and N3 to interact with the atom Br3, and to the hydrogens bound to N5 and N6 to interact with the atom Br1 (see Table 2 for the H-bond distances and angles).

Table 2
H-bond distances (Å) and angles (°) for **L1**·6HBr

O1–H1	H1···Br2	O1–H1···Br2
1.2(1)	2.1(1)	162(10)
N2–H2b	H2b···Br3	N2–H2b···Br3
0.900(5)	2.362(1)	168.6(4)
N3–H3a	H3a···Br3	N3–H3a···Br3
0.890(7)	2.617(1)	160.1(1)
N3–H3b	H3b···Br6	N3–H3b···Br6
0.890(7)	2.421(1)	150.8(4)
N3–H3c	H3c···Br4	N3–H3c···Br4
0.890(7)	2.406(1)	157.1(5)
N4–H4a	H4a···Br5	N4–H4a···Br5
0.900(6)	2.358(1)	170.0(4)
N5–H5a	H5a···Br1	N5–H5a···Br1
0.900(7)	2.395(1)	164.0(4)
N6–H6a	H6a···Br1	N6–H6a···Br1
0.890(8)	2.520(1)	166.1(5)
N1–H1a	H1a···Br3^{1}	N1–H1a···Br3^{1}
0.900(6)	2.515(1)	140.1(4)
N1–H1b	H1b···Br2^{2}	N1–H1b···Br2^{2}
0.900(6)	2.293(1)	179.9(4)
N2–H2a	H2a···Br1^{3}	N2–H2a···Br1^{3}
0.900(6)	2.447(1)	144.9(4)
N4–H4b	H4b···Br1^{1}	N4–H4b···Br1^{1}
0.900(6)	2.619(1)	137.5(4)
N5–H5b	H5b···Br4^{5}	N5–H5b···Br4^{5}
0.900(6)	2.507(1)	137.9(4)
N6–H6b	H6b···Br4^{6}	N6–H6b···Br4^{6}
0.890(7)	2.462(1)	151.3(5)
N6–H6c	H6c···Br6^{4}	N6–H6c···Br6^{4}
0.890(7)	2.484(1)	166.4(5)

Equivalent positions: $^{1}x+1, y, z$; $^{2}-x+1, -y+1, -z$; $^{3}-x, -y+1, -z$; $^{4}x, y, z-1$; $^{5}-x, -y, -z$; $^{6}x-1, y, z-1$.

In conclusion, regarding the dispositions of the side chains, it was found that the two chains lie in opposite regions of space with respect to the plane containing the aromatic ring (see Fig. 2).

Finally, many short hydrogen bonds (in addition to those reported above) are present in the crystal lattice. These interactions involve the hydrogen atoms of the $[H_6\mathbf{L1}]^{6+}$ cation and the bromide anions (see Table 2).

3.3. Solution studies

3.3.1. Acid–base properties

Table 3 summarizes the basicity constants of **L1** and **L2** as determined potentiometrically in 0.15 mol dm^{-3} NaCl aqueous solution at 298.1 K. The neutral compound **L1** behaves as a monoprotic acid and as hexaprotic base, while the neutral **L2** behaves as a diprotic acid and as hexaprotic base under the experimental conditions used. As shown in Table 3, both neutral species of **L1** and **L2** can achieve, in solution, the

Table 3
Equilibrium constants (298.15 K, $I = 0.15$ mol dm^{-3}, NaCl) for the protonation equilibria of **L1** and **L2** in aqueous solution

Reaction	Log K	
	L1	**L2**
$H_{-2}L^{2-} + H^+ = H_{-1}L^-$		10.50(2) [a]
$H_{-1}L^- + H^+ = L$	10.87 (1)	10.38 (2)
$L + H^+ = HL^+$	10.22 (2)	9.69 (2)
$HL^+ + H^+ = H_2L^{2+}$	9.42 (1)	9.23 (1)
$H_2L^{2+} + H^+ = H_3L^{3+}$	9.00 (1)	8.22 (1)
$H_3L^{3+} + H^+ = H_4L^{4+}$	6.10 (1)	7.44 (1)
$H_4L^{4+} + H^+ = H_5L^{5+}$	4.31 (2)	4.40 (2)
$H_5L^{5+} + H^+ = H_6L^{6+}$	3.64 (1)	3.75 (3)

[a] Values in parentheses are the standard deviations on the last significant figure.

anionic species $H_{-1}\mathbf{L1}^-$ and $H_{-2}\mathbf{L2}^{2-}$, respectively, indicating the removal of the acidic hydrogens of the aromatic moieties; moreover, both ligands can be fully protonated in acidic solution reaching the H_6L^{6+} species in which all six amine functions are protonated. By analyzing the protonation constants of the two ligands, some general aspects can be outlined; it was found that both ligands show very similar basicity in many protonation steps, due to the very similar structures of both compounds. In fact, taking into account that **L2** shows, for its topology, the first protonation to the $H_{-2}\mathbf{L2}^-$ species, both ligands exhibit approximately the same logarithmic values for the protonation constants as many of the same speciation (see Table 3). Specifically, the values of the addition constants from the first to the fourth protonation steps of **L1** are similar to those, from the second to the fifth, of **L2**; they show a slight decrease in the $\log K$ values ranging from $\log K_1 = 10.87$ to $\log K_4 = 9.00$ and from $\log K_2 = 10.38$ to $\log K_5 = 8.22$ for **L1** and **L2**, respectively. Again, the values of $\log K$ in the last two protonation steps are similar for both compounds. The only significant difference is the drop by three logarithmic units that in **L1** appears in the addition of H^+ to the H_3L^{3+} species, while a similar drop occurs in the addition to H_4L^{4+} species for **L2**. This aspect can be explained taking into account that **L2** has one more protonable site than **L1**. In fact, considering the number of protonation sites and their localization in both ligand, these trends in the constant values can be easily explained in terms of minimization of the electrostatic repulsion between positive charges in the protonated species.

In other words, the first four protons can occupy positions far from each other and thus experience little charge repulsion in **L1**, while this is possible up to the sixth proton for **L2**, also considering that the phenolic moieties play an important role in the protonation steps by forming a hydrogen bond network with the amine functions in benzyl position.

The first four constant values in **L1** suggest that the two polyamine sub-units should be involved in these proton additions, while the phenol is only involved in the fifth step. On the contrary, more effects need to be taken into account in the case of **L2**.

The UV–Vis absorption electronic spectra of **L1** and **L2** in aqueous solutions with different pH values gave further information about the role of the phenolic function in the acid–base behavior of both ligands. The absorption parameters are reported in Table 6. The spectra, recorded at different pH, show different features in the acidic or alkaline pH range for both ligand; at acid pH, a λ_{max} at 277 nm or at 265 is observable for **L1** and **L2**, respectively, while at alkaline pH, two bands with λ_{max} at 240 and 293 nm appear in the spectra of **L1** and only one band with λ_{max} at 296 appears in the spectra of **L2**. This different spectral behavior in the opposite field of pH is characteristic of the phenolic function, which, depending on the pH values, is present in phenol or phenolate form. In other words, the change in λ_{max} is due to the presence of the phenol hydroxyl form at low pH values and to the phenolate form at higher pH. It is to underline the values of the molar absorptivity parameter (ε) which was found to be more than six times higher for the species of **L2** than for those of **L1** (see Table 6). Fig. 3 (top) shows the trend of the band with $\lambda_{max} = 293$ nm as a function of pH together with the distribution diagram of the protonated species of **L1**; Fig. 3 (bottom) reports the same trend due to the band with $\lambda_{max} = 296$ in the case of **L2**. Monitoring the spectra from acid to alkaline pH, the increase in absorbance at 293 nm, in the case of **L1**, starts from pH values higher than 4 and maximum absorbance is reached at pH 6 (see Fig. 3). This indicates that deprotonation of the phenol occurs in the H_4L^{4+} species, in agreement with the potentiometric data; in this species, and in the species present at higher pH values, the acidic protons must therefore be positioned mainly on the amine functions. The trend observed for **L2** is more complicated, in that the band with $\lambda_{max} = 296$ starts to appear at pH values higher than 6 associated with the formation of the $H_3\mathbf{L}^{3+}$ species and rapidly increases up to pH 8, where the $H_3\mathbf{L}^{3+}$ species is completely formed, then further increases up to pH 10.5, but with a different slope. This trend can be interpreted taking into consideration that two deprotonation steps are possible for the BPH moieties, and thus one deprotonation occurs in the H_3L^{3+} species, while the second is probably shared on the species present at pH higher than 8. However, both deprotonation steps of the BPH group of **L2** occur at pH higher than that of the PH group in **L1**, suggesting a lower acidity of BPH with respect to the PH group.

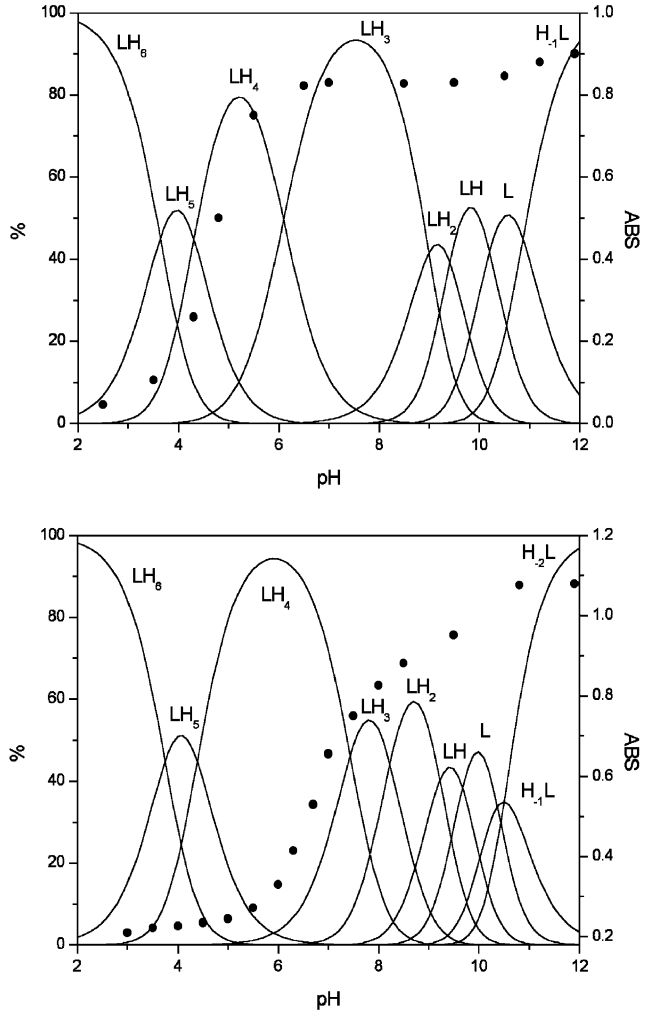

Fig. 3. Absorbance values at $\lambda = 293$ nm (●) and distribution diagram of the protonated species (---) of **L1** (top), absorbance values at $\lambda = 296$ nm (●) and distribution diagram of the protonated species (---) of **L2** (bottom) as a function of pH, in aqueous solution at 298.1 K in 0.15 mol dm^{-3} NaCl.

3.3.2. Coordination of metal ions

The coordination behavior of **L1** and **L2** towards the bipositive metal cations Cu(II), Zn(II), and Cd(II) was potentiometrically studied in 0.15 mol dm^{-3} NaCl aqueous solution at 298.1 K and the data are reported in Tables 4 and 5. Both ligands form stable mono- and dinuclear complexes with all the metal ions investigated.

When the metal to ligand ratio is close to 1:1, the mononuclear species is largely prevalent in solution, although they coexist with the dinuclear one; when the **L**/M(II) molar ratio is 1:2, the dinuclear species are instead prevalent. This behavior is depicted in Fig. 4(a) and (b), and in Fig. 5(a) and b for the complexed species of Cu(II) with **L1** and **L2**, respectively. Fig. 5(a) and (b) report the distribution diagrams of the species in the system **L**/Cu(II) in 1:1 and 1:2 molar ratios, respectively, as a function of pH.

Table 4
Equilibrium constants (298.15 K, $I = 0.15$ mol dm^{-3}, NaCl) for the metal complex equilibria of **L1** in aqueous solution

Reaction	Log K		
	Cu	Zn	Cd
$M+H_{-1}L = MH_{-1}L$ [a]	22.32 (2) [b]	13.38 (2)	12.27 (4)
$M+H_{-1}L+H = ML$	31.84 (2)	24.01 (2)	22.54 (3)
$M+H_{-1}L+2H = MLH$	40.40 (2)	32.35 (1)	30.24 (1)
$M+H_{-1}L+3H = MLH_2$	44.64 (3)	37.34 (2)	36.42 (3)
$M+H_{-1}L+4H = MLH_3$	48.48 (4)	–	–
$M+H_{-1}L+H_2O = M(H_{-1}L)OH+H$	12.25 (2)	2.82	1.27 (5)
$M+H_{-1}L+2H_2O = M(H_{-1}L)(OH)_2+2H$	0.96 (3)	–	–
$2M+H_{-1}L+H = M_2L$	42.36 (3)	–	–
$2M+H_{-1}L = M_2H_{-1}L$	38.73 (3)	22.80 (3)	19.28 (3)
$2M+H_{-1}L+H_2O = M_2(H_{-1}L)OH+H$	28.81 (3)	15.74 (3)	8.49 (5)
$MH_{-1}L+H = ML$	9.52	10.63	10.27
$ML+H = MLH$	8.56	8.34	7.7
$MLH+H = MLH_2$	4.24	4.99	6.18
$MLH_2+H = MLH_3$	3.84	–	–
$MH_{-1}L+OH = M(H_{-1}L)OH$	3.76	3.17	2.83
$M(H_{-1}L)OH+OH = M(H_{-1}L)(OH)_2$	2.54	–	–
$M+MH_{-1}L = M_2H_{-1}L$	16.41	9.42	7.01
$M_2H_{-1}L+OH = M_2(H_{-1}L)OH$	3.81	6.77	3.04

[a] Charges are omitted for clarity.
[b] Values in parentheses are the standard deviations on the last significant figure.

3.3.2.1. Mononuclear complexes. **L1** and **L2** form stable mononuclear complexes with the metal ions examined here. The Cu(II) complexes show higher stability than the Zn(II) and Cd(II) complexes for both ligands.

Table 5
Equilibrium constants (298.15 K, $I = 0.15$ mol dm^{-3}, NaCl) for the metal complex equilibria of **L2** in aqueous solution

Reaction	Log K		
	Cu	Zn	Cd
$M+H_{-2}L = MH_{-2}L$ [a]	22.10 (3) [b]	13.50 (1)	11.59 (4)
$M+H_{-2}L+H = MH_{-1}L$	31.74 (2)	23.05 (3)	21.20 (4)
$M+H_{-2}L+2H = ML$	41.01 (1)	32.50 (4)	29.99 (6)
$M+H_{-2}L+3H = MLH$	48.92 (2)	40.63 (2)	38.18 (2)
$M+H_{-2}L+4H = MLH_2$	53.83 (1)	–	44.43 (4)
$2M+H_{-2}L+H = M_2H_{-1}L$	46.00 (2)	–	–
$2M+H_{-2}L = M_2H_{-2}L$	41.79 (3)	24.55 (3)	19.46 (4)
$2M+H_{-2}L+H_2O = M_2(H_{-2}L)OH+H$	30.70 (5)	15.02 (3)	8.80 (3)
$MH_{-2}L+H = MH_{-1}L$	9.64	9.55	9.61
$MH_{-1}L+H = ML$	9.27	9.45	8.79
$ML+H = MLH$	7.91	8.13	8.19
$MLH+H = MLH_2$	4.91	–	6.25
$M+MH_{-2}L = M_2H_{-2}L$	19.69	11.05	7.87
$M_2H_{-1}L+OH = M_2(H_{-1}L)OH$	2.74	4.3	3.17

[a] Charges are omitted for clarity.
[b] Values in parentheses are the standard deviations on the last significant figure.

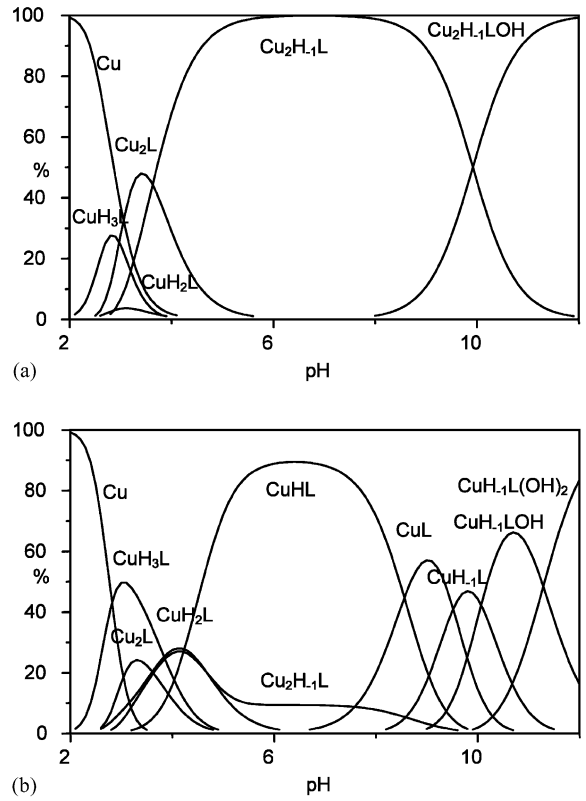

Fig. 4. Distribution diagrams of the species for the system **L1**/Cu(II) as a function of pH in aqueous solution, $I = 0.15$ mol dm^{-3} NaCl, at 298.1 K. (a) [**L1**] $= 1 \times 10^{-3}$ mol dm^{-3}, [Cu^{2+}] $= 1 \times 10^{-3}$ mol dm^{-3}; (b) [**L1**] $= 1 \times 10^{-3}$ mol dm^{-3}, [Cu^{2+}] $= 2 \times 10^{-3}$ mol dm^{-3}.

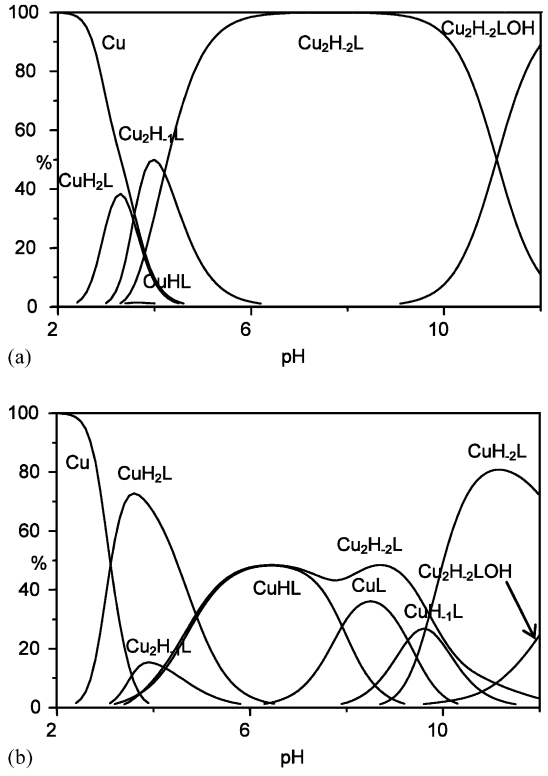

Fig. 5. Distribution diagrams of the species for the system **L2**/Cu(II) as a function of pH in aqueous solution, $I = 0.15$ mol dm^{-3} NaCl, at 298.1 K. (a) [**L2**] $= 1 \times 10^{-3}$ mol dm^{-3}, [Cu^{2+}] $= 1 \times 10^{-3}$ mol dm^{-3}; (b) [**L2**] $= 1 \times 10^{-3}$ mol dm^{-3}, [Cu^{2+}] $= 2 \times 10^{-3}$ mol dm^{-3}.

Comparison of the stability constants of the complexation reactions of the same M(II) ion to the fully deprotonated species (H_{-1}**L1**$^{-}$ and H_{-2}**L2**$^{2-}$, respectively) of the two ligands showed that the addition of all the three metal ions to such species is approximately equal for both ligands (Tables 4 and 5). These data suggest that both ligands participate in the coordination of the same metal ions with the same donor atoms, giving rise to similar coordination patterns. Taking into account the molecular framework of the ligands and the higher values of the stability constants compared with the stability constants of the same metal ions coordinated by the dien ligand [28], it can be supposed that at least four donor atoms are involved in the stabilization of the metal ions: three amine functions of one of the dien sub-units and the oxygen of the phenolate groups.

This hypothesis is in agreement with the stability constants of the same metal complexes with **L3** in which three amine atoms and one phenolate oxygen atom were presumed to be involved in the coordination pattern. Moreover, the presence of several protonated species and the values of the addition constants of the protons to the complexed species support this hypothesis. In fact, these values are similar to those for the addition of the proton to the free ligands; for example, the additions of the first three protons to the species [MH_{-2}**L2**] have values close to those of the first three proton additions to the free ligands. The same argument can be made for **L1**, except in the case of the Cd(II) ion where a slight further involvement of an additional nitrogen atom cannot be excluded, the latter given the higher dimension of Cd(II) ion, which probably permits the other flexible subunit to interact with the metal.

In conclusion, it can be stated that in almost all the metal-complexed species [MH_{-1}**L1**]$^{+}$ or [MH_{-2}**L2**], one of the amine sub-units together with the phenolate oxygen is involved in the coordination of the metal ions, while the other sub-unit remains not involved in the coordination.

3.3.2.2. Dinuclear complexes. Both ligands form stable dinuclear complexes with the three metal ions. The [MH_{-1}**L1**]$^{+}$ as well as the [MH_{-2}**L2**] species can coordinate another M(II) ion in aqueous solution, giving the dinuclear species with [M_2H_{-1}**L1**]$^{3+}$ and [M_2H_{-2}**L2**]$^{2+}$ stoichiometry, respectively. In the case of **L1**, the constant values for the addition of the second cation to the mononuclear species are lower than those for the addition of the first one, while they are

approximately the same in the case of **L2**. This aspect can be explained considering the topology of the ligands. In **L2** the triamine sub-units are separated by the long spacer BPH, while in **L1** they are obviously closer. In the case of **L2** there are two identical but separate binding areas, each formed by one of the triamine sub-units and by the oxygen of the phenol group; for this reason, the two cations are probably coordinated far from each other with the same coordination environment. This is not however possible in the $[M_2H_{-1}\mathbf{L1}]^{3+}$ species, where the two coordinated cations are necessarily closer and each suffers from the presence of the other one, giving rise to a decrease in the addition constant of the second metal ion. However, the quite high values for the second metal addition, suggest a tetra-coordination environment also for this second metal ion; in that case, the two metals would have similar coordination environments characterized by a phenol oxygen bridging the two cations. This hypothesis is supported by the similar addition constants of the second M(II) ions found for the same species $[MH_{-1}L]^{+}$ of **L3**, where it was demonstrated that the phenolate oxygen acts as bridging ligand between the two metal ions. In other words, it is likely that with **L1** the two metals are each coordinated by one tri-amine sub-unit and by the oxygen of the phenolate which bridges the two metals forcing them to stay close to each other. On the contrary, with **L2** the two metals again show the same coordination skeleton as in **L1**, but in this case it is formed by the tri-amine sub-unit and by the oxygen atom of the closest phenolate group; in this way, the two cations are located far from each other.

UV spectra were recorded in aqueous solution containing **L1** or **L2** and M(II) in various molar ratios and different pH values in order to understand the role played by the phenolic function in the formation of the complexes. Only the results obtained in the pH range where only one species is prevalent in solution are reported.

For example, with regard to the spectra for the system **L1**/Cu(II) in a 1:1 molar ratio, the spectrum recorded at pH 6.5, where the $[CuH_2\mathbf{L1}]^{4+}$ species is prevalent in solution, shows four bands at λ_{max} 242, 278, 386, and 609 nm, respectively (Table 6). The two bands at higher energy are due to the π–π^* transitions of the phenolate group, the band at 386 nm is ascribed to the phenolate–copper charge transfer [29], and the other band to the copper d–d electron transfer. These data indicate the involvement of the oxygen of the aromatic chromophore as phenolate in the stabilization of this species, which occurs at acidic pH values. These spectral data do not substantially change even at higher pH values. Similar features were found for the complexes of Cu(II) with **L2**, although with different absorption energies, and also for the other two metal complexes of both ligands which, however, cannot show the diagnostic band of phenol–metal electron transfer (see Table 6). Thus, in the mononuclear metal complexes of both ligands it would appear that the phenolic group of **L1** and one of those of **L2**, always participate in the coordination in its phenolate form starting from the protonated species.

Similar results were also obtained in the spectra recorded with **L**/M(II) in a 1:2 molar ratio. In the spectra recorded for the dinuclear complexes of **L2** at

Table 6
Characteristics of the UV–Vis spectra (λ_{max} (nm) and $\varepsilon_{\lambda max}$($mol^{-1}$ dm^3 cm^{-1})) of compounds **L1** and **L2**, in aqueous solution at pH 2, 12, and of their metal complexes

$H_6\mathbf{L1}^{6+}$		$H_{-1}\mathbf{L1}^{-}$		$H_6\mathbf{L2}^{6+}$		$H_{-2}\mathbf{L2}^{2-}$					
λ_{max}	ε	λ_{max}	ε	λ_{max}	ε	λ_{max}	ε				
277	3000	240	7100	265	19 650	296	26 750				
		293	4200								
[CuH**L1**] [a]		[CuH$_{-2}$**L2**]		[ZnH**L1**]		[ZnH$_{-2}$**L2**]		[Cd**L1**]		[CdH$_{-2}$**L2**]	
λ_{max}	ε	λ_{max}	ε	λ_{max}	ε	λ_{max}	ε	λ_{max}	ε	λ_{max}	ε
242	8200	288	32 600	244	6300	291	28 300	239	5800	296	28 600
278	6400	391	850	288	4500			291	3600		
386	600	589	230								
609	180										
[Cu$_2$H$_{-1}$**L1**]		[Cu$_2$H$_{-2}$**L2**]		[Zn$_2$H$_{-1}$**L1**]		[Zn$_2$H$_{-2}$**L2**]		[Cd$_2$H$_{-1}$**L1**]		[Cd$_2$H$_{-2}$**L2**]	
λ_{max}	ε	λ_{max}	ε	λ_{max}	ε	λ_{max}	ε	λ_{max}	ε	λ_{max}	ε
242	8200	295	25 000	239	5850	289	28 900	239	6000	294	29 050
281	6400	391	1600	283	3100			289	3800		
384	1100	589	450								
604	350										

[a] Charges are omitted for clarity.

pH value where the $[M_2(H_{-2}\mathbf{L2})]^{2+}$ or $[M_2(H_{-2}\mathbf{L2})OH]^{+}$ species are prevalent in solution (these species are the only existing in solution over pH 8), one band was detected for the interaction of light with the aromatic moieties producing π–π* transitions having values of λ_{max} 295 for Cu(II), 289 for Zn(II) and 294 nm for the Cd(II) complex, respectively (see Table 6). Again, this feature indicates an involvement of the oxygen of the aromatic groups as phenolate in the stabilization of the metal ions coordinated in the dinuclear species.

Electronic absorption spectra in the visible region give further information regarding the Cu(II) complexes; the spectrum of the dinuclear $[Cu_2(H_{-2}\mathbf{L2})]^{2+}$ complexes again shows two more bands with λ_{max} 391 and 589 nm, as below, due to phenolate-to-metal charge transfer and to the d–d electron transfer of Cu(II), respectively, confirming the involvement of the phenolate group in the coordination of the two metal ions. Moreover, in this molar ratio, the molar absorptivity parameter is higher than that found for the mononuclear $[CuH_{-2}\mathbf{L2}]$ species, underlining that each phenolate group is involved in the coordination of one Cu(II) ion of the dinuclear complexes.

Similar spectral features were found for the Cu(II) dinuclear species of **L1**, although no strong increase in the molar absorptivity parameter of the band around 390 nm was found, due to the presence of only one phenolate group. Moreover, the UV range preserves this spectral feature in the dinuclear complexes of **L2** with the other two metal ions and in those of **L1**, again highlighting the involvement of the group in coordination (see Table 6). Again, it should be underlined that there is a strong difference in the molar absorptivity parameter for the PH and the BPH groups also in the metal complexes, in which this value was found to be approximately six times higher for BPH than PH.

In conclusion, the studies in aqueous solution highlighted the ability of both ligands to form stable dinuclear complexes, and the important role played by the phenolic group. The dinuclear $[M_2(H_{-2}\mathbf{L2})]^{2+}$ and $[M_2(H_{-2}\mathbf{L2})OH]^{+}$ species for **L2** and $[M_2(H_{-1}\mathbf{L1})]^{3+}$ and $[M_2(H_{-1}\mathbf{L1})OH]^{2+}$ species for **L1** appear to be virtually the only species existing in solution for L/M(II) molar ratio of 1:2 over pH 6.

The dinuclear species formed by the same ligands with the three metal ions have a similar coordination arrangements; instead, the environment is different for the same metal dinuclear complexes formed by different ligands. In particular, in the dinuclear $[M_2(H_{-1}L)]^{3+}$ species of **L1**, the coordination pattern for each metal ion is formed by the dien sub-unit and by the oxygen of the phenolate which bridges the two metals bringing them close to each other. On the contrary, in the dinuclear $[M_2(H_{-2}L)]^{2+}$ species of **L2**, the coordination pattern for each metal ion is again due to the dien sub-unit and by oxygen of the phenolate which, in this case, interacts with only one metal. In this way, the two metals are far from each other, and two coordination areas, which act independently in the coordination of the metal ions, can be found in **L2**. A proposal for the coordination sites in the dinuclear complexes, is shown in Fig. 6(a) and (b). However, all the dinuclear species show an unsaturated coordination sphere which can be completed by adding new species from the medium, such as water molecules or the OH^- anion. In the case of **L1** the two metals can cooperate to bind substrates, while they can act independently in the dinuclear species of **L2**.

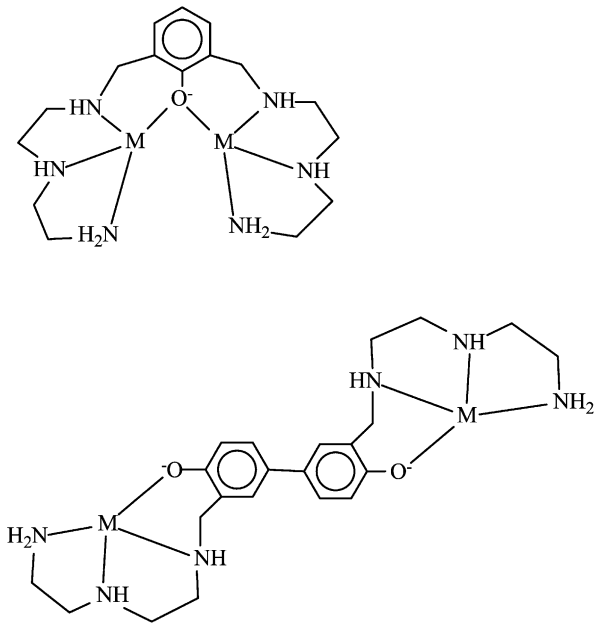

Fig. 6. Proposed coordination modes for the Cu(II), Zn(II), and Cd(II) ions in (a) $[M_2H_{-1}\mathbf{L1}]^{3+}$ and (b) $[M_2H_{-2}\mathbf{L2}]^{2+}$ complexes.

4. Conclusions

The synthesis of two new ligands bearing two triamine functions separated by two different phenolic groups was obtained. In the case of **L1** the synthesis foresees a multi-step scheme, while **L2** was obtained directly in a one-pot reaction. The insertion of two different rigid spacers (PH in **L1**, BPH in **L2**) bearing donor atoms to separate the two triamine units produces changes in the coordination properties of the two ligands towards the metal cations Cu(II), Zn(II) and Cd(II) studied; the main difference is an increased compartmental behavior of **L2** as compared to **L1**. The mononuclear species formed with the fully deprotonated ligands show similar formation constants for both ligands in relation to the same M(II) ions, but these

values are always higher for the dinuclear complexes of **L2** than **L1**. This result is ascribed to the different topology of the two ligands; in fact, the coordination pattern in the mononuclear species of both ligands is formed by one tri-amine moiety and one phenolate oxygen. This coordination pattern is also preserved in the dinuclear species but with a different disposition of the two metal ions in the complex. In the dinuclear complexes formed with the $H_{-1}\mathbf{L1}^{-}$ species, the same coordination pattern is reached by the phenolate oxygen bridging the two metals; this is possible in that the two tri-amine moieties are linked to the phenolic group. This means that the two metal ions must be close to each other in the complex and thus reciprocally suffer from each others charge. The same coordination pattern is also preserved in the dinuclear species of $H_{-2}\mathbf{L2}^{2-}$ species, but in this case, because the tri-amine functions are far from each other, the oxygen of each phenolate interacts with one metal only and as a result the two metals will be displaced far from each other and not interact. Thus, two coordination areas, which act independently in the coordination of the metal ions, can be found in **L2**. In all the dinuclear complexes, however, the metal ions show an unsaturated coordination environment; for this reason, these species should be able to bind at least another ligand, giving rise to *cascade complexes*. The two metal centers of **L2** are able to bind substrates independently, while the metal centers in **L1** can cooperate in order to saturate their coordination requirement.

5. Supplementary material

X-ray crystallographic files in CIF format for the structure $[H_6\mathbf{L1}]\cdot 6Br$ have been deposited with the Cambridge Crystallographic Data Centre, CCDC No. 198066. Copies of this information may be obtained free of charge from The Director, CCDC, 12 Union Road, Cambridge, CB2 1EZ, UK (fax: +44-1223-336033; e-mail: deposit@ccd.cam.ac.uk or www: http://www.ccdc.cam.ac.uk).

Acknowledgements

Financial support from the Italian Ministero dell'Istruzione, dell'Università e della Ricerca (PRIN2002) is gratefully acknowledged.

References

[1] (a) C.J. Pedersen, J. Am. Chem. Soc. 89 (1967) 7017;
(b) J.M. Lehn, Pure Appl. Chem. 49 (1977) 857;
(c) D.J. Cram, J.M. Cram, Science 183 (1984) 4127;
(d) J.M. Lehn, Angew. Chem., Int. Ed. Engl. 27 (1988) 89.

[2] (a) A. Bianchi, K. Bowman-James, E. Garcia-España (Eds.), Supramolecular Chemistry of Anions, Wiley-VCH, New York, 1997;
(b) J.M. Lehn, Supramolecular Chemistry, Concepts and Perspectives, VCH, Weinheim, 1995.

[3] (a) P. Guerriero, S. Tamburini, P.A. Vigato, Coord. Chem. Rev. 110 (1995) 17;
(b) C. Bazzicalupi, A. Bencini, V. Fusi, C. Giorgi, P. Paoletti, B. Valtancoli, Inorg. Chem. 37 (1998) 941 (and references therein).

[4] (a) H. He, A.E. Martell, R.J. Motekaitis, J.J. Reibespiens, Inorg. Chem. 39 (2000) 1586;
(b) T. Koike, M. Inoue, E. Kimura, M. Shiro, J. Am. Chem. Soc. 118 (1996) 3091.

[5] (a) C. Bazzicalupi, A. Bencini, A. Bianchi, V. Fusi, E. Garcia-España, C. Giorgi, J.M. Llinares, J.A. Ramirez, B. Valtancoli, Inorg. Chem. 38 (1999) 620 (and references therein);
(b) F. Meyer, R.F. Winter, E. Kaifer, Inorg. Chem. 40 (2001) 4597.

[6] (a) S.J. Lippard, J.M. Berg, Principles of Bioinorganic Chemistry, University Science Books, Mill Valley, CA, 1994;
(b) J. Reedijk (Ed.), Bioinorganic Catalysis, Marcel Dekker, New York, 1993;
(c) V. Fusi, A. Llobet, J. Mahia, M. Micheloni, P. Paoli, X. Ribas, P. Rossi, Eur. J. Inorg. Chem. 4 (2002) 987.

[7] (a) K.D. Karlin, Science 261 (1993) 701;
(b) D.E. Wilcox, Chem. Rev. 96 (1996) 2435;
(c) M.N. Hughes, The Inorganic Chemistry of the Biological Processes, Wiley, New York, 1981.

[8] (a) Y.L. Agnus, Copper Coordination Chemistry: Biochemical and Inorganic Perspective, Adenine Press, New York, 1983;
(b) I. Bertini, C. Luchinat, W. Marek, M. Zeppezauer (Eds.), Zinc Enzymes, Birkhauser, Boston, MA, 1986.

[9] (a) A.E. Martell, D.T. Sawyer, Oxygen Complexes and Oxygen Activation by Transition Metals, Plenum Press, New York, 1987;
(b) S. Schindler, Eur. J. Inorg. Chem. (2000) 2311;
(c) M.B. Davies, Coord. Chem. Rev. (1996) 1;
(d) S. Aoki, E. Kimura, J. Am. Chem. Soc. 122 (2000) 4542;
(e) N. Ceccanti, M. Formica, V. Fusi, M. Micheloni, R. Pardini, R. Pontellini, M.R. Tinè, Inorg. Chim. Acta 321 (2001) 153.

[10] (a) F. Meyer, P. Rutsch, Chem. Commun. (1998) 1037;
(b) P.A. Karplus, M.A. Pearson, R.P. Hausinger, Acc. Res. Chem. 30 (1997) 330;
(c) M. Musiani, E. Arnolfi, R. Casadio, S. Ciurli, J. Biol. Inorg. Chem. 6 (2001) 300.

[11] (a) C.J. Cooksey, P.J. Garratt, E.J. Land, S. Pavel, C.A. Ramsden, P.A. Riley, N.P.M. Smit, J. Biol. Chem. 272 (1997) 26226;
(b) L.M. Sayre, D.V. Nadkarni, J. Am. Chem. Soc. 116 (1994) 3157;
(c) A. Sánchez-Ferrer, J.N. Rodríguez-López, F. García-Cánovas, F. García-Carmona, Biochim. Biophys. Acta 1247 (1995) 1.

[12] (a) A.M. Barrios, S.J. Lippard, J. Am. Chem. Soc. 122 (2000) 9172;
(b) A.M. Barrios, S.J. Lippard, Inorg. Chem. 40 (2001) 1250.

[13] (a) P. Dapporto, M. Formica, V. Fusi, M. Micheloni, P. Paoli, R. Pontellini, P. Rossi, Inorg. Chem. 39 (2000) 4663;
(b) P. Dapporto, M. Formica, V. Fusi, M. Micheloni, P. Paoli, R. Pontellini, P. Rossi, Inorg. Chem. 40 (2001) 6186–6192;
(c) P. Dapporto, M. Formica, V. Fusi, M. Micheloni, P. Paoli, R. Pontellini, P. Rossi, Supramol. Chem. 13 (2001) 369.

[14] M. Formica, L. Giorgi, V. Fusi, M. Micheloni, R. Pontellini, Polyhedron 21 (2002) 1351 (and references therein).

[15] M. Formica, V. Fusi, L. Giorgi, M. Micheloni, P. Palma, R. Pontellini, Eur. J. Org. Chem. 1 (2002) 402.

[16] O.J. Gelling, B.L. Feringa, J. Am. Chem. Soc. 112 (1990) 7599.
[17] A.R. Jacobson, S.W. Tam, L.M. Sayre, J. Med. Chem. 34 (1991) 2816.
[18] A. Altomare, G.L. Cascarano, C. Giacovazzo, A. Guagliardi, M.C. Burla, G. Polidori, M. Camalli, M. J. Appl. Cryst. 32 (1999) 115.
[19] G.M. Sheldrick, SHELX 97, University of Göttingen, Göttingen, Germany, 1997.
[20] N. Walker, D.D. Stuart, Acta Crystallogr., Sect. A 39 (1993) 158.
[21] M. Nardelli, Comput. Chem. 7 (1983) 95.
[22] L.J. Farrugia, J. Appl. Cryst 30 (1997) 565.
[23] M. Fontanelli, I Spanish-Italian Conference Thermodynamics of Metal Complexes, Peñiscola, June 3–6, University of Valencia, Spain, (1990) 41.
[24] (a) G. Gran, Analyst 77 (1952) 661;
(b) F.J. Rossotti, H. Rossetti, J. Chem. Educt. 43 (1996) 1739.
[25] P. Gans, A. Sabatini, A. Vacca, Talanta 43 (1996) 1739.
[26] +sc = syn-clinal: +30° to +90°; -sc = syn-clinal: −30° to −90°; ±ap = anti-periplanar: +150°–210° (or −150°); +ac = anti-clinal: +90° to +150°.
[27] W. Klyne, V. Prelog, Experientia 19 (1960) 521.
[28] IUPAC Stability Constant (SD-Database), Academic Software, 2001, Version 5.14.
[29] K.D. Karlin, P. Ghosh, R.W. Cruse, A. Farooq, Y. Gultneh, R.R. Jacobson, N.J. Blackburn, R.W. Strange, J. Zubieta, J. Am. Chem. Soc. 110 (1988) 6769.